

# Micro-Displacement Sensor Based on High Sensitivity Photonic Crystal

Saeed OLYAEE\* and Morteza AZIZI

*Nano-Photonics and Optoelectronics Research Laboratory (NORLab), Faculty of Electrical and Computer Engineering, Shahid Rajaee Teacher Training University (SRTTU), 16788-15811, Tehran, Iran*

\*Corresponding Author: Saeed OLYAEE      E-mail: s\_olyaee@srttu.edu

**Abstract:** In this paper, we present a micro-displacement sensor formed by the fixed and movable photonic crystal slabs. In this sensor, a waveguide was created by changing the radius of holes rather than removing them. At a proper operating wavelength, the structure could be used as the micro-displacement sensor. The results revealed that the micro-displacement sensor had a sensitivity of  $3.6 \mu\text{m}^{-1}$ , the  $Q$ -factor was nearly 180, and the sensing range was  $0.0 \mu\text{m} - 0.5 \mu\text{m}$ . The properties of the micro-displacement sensor are also analyzed theoretically and verified using the finite-difference time-domain (FDTD) method carried out using the software (Rsoft).

**Keywords::** Micro-displacement sensor,  $Q$ -factor, waveguide, sensitivity, FDTD, Lorentzian function

---

Citation: Saeed OLYAEE and Morteza AZIZI, "Micro-Displacement Sensor Based on High Sensitivity Photonic Crystal," *Photonic Sensors*, 2014, 4(3): 220–224.

---

## 1. Introduction

The micro-displacement sensor is an important measurement system in many applications such as the micro-electro-mechanical systems (MEMS), aerospace, structure health monitoring, and many engineering fields [1, 2]. Many efforts are being devoted to measure the displacement with the high accuracy by using the photonic crystal (PhC) sensors and laser interferometers [3–5]. The photonic crystal structure is one of the most useful devices for the sensing systems [6, 7]. Over the past few decades, these devices were considered for sensing applications. These devices have very useful features such as the small size, high sensitivity, and wide range of wavelengths. Various designs of the micro-sensor based on the PhCs have been proposed recently. A sensor based on the PhC waveguide

which can provide a sensitivity of  $1 \mu\text{m}^{-1}$ , was introduced by Levy *et al.* in 2005 [3]. This sensor needs three detectors to be used, which does not only complicate the structure of a micro-sensor, but also the error in any of the detectors will deteriorate the measurement results [2]. Another sensor was introduced in 2006 by Xu *et al.* [1]. This sensor is based on the line-defect resonant cavity in the PhC which can provide a sensitivity of about  $1 a^{-1}$  ( $a$  is the lattice constant) [1]. This sensor needs only one detector, the line-defect resonant cavity structure of the device is simple, and the  $Q$ -factor is only 40 [2]. The next sensor was introduced in 2007 by Xu *et al.* [8]. They proposed a micro-displacement sensor with a large dynamic range, and its sensing technique is based on a PhC co-directional coupler. Another displacement sensor was presented in 2011 by Yang *et al.* [2]. This sensor can provide a

---

Received: 3 March 2014 / Revised version: 22 May 2014

© The Author(s) 2014. This article is published with open access at Springerlink.com

DOI: 10.1007/s13320-014-0183-2

Article type: Regular

sensitivity of about  $1 a^{-1}$  with the  $Q$ -factor of 6000.

In this paper, we propose a micro-displacement sensor formed by the fixed and movable photonic crystal segments. The sensitivity and  $Q$ -factor of this sensor were  $3.6 a^{-1}$  and 180, respectively. The properties of the micro-displacement sensor are analyzed theoretically and verified using the finite-difference time-domain (FDTD) method.

## 2. Theoretical analysis of the designed sensor

Figure 1 shows the designed sensor layout. This sensor includes two coplanar PhC segments; one of them is fixed, and the other is movable. These segments are aligned along a common axis. The light emitted from the light source propagates through the waveguide, and the transmission intensity is detected by a photodetector. When the distance between two PhC segments is changed, the transmission intensity will change. In a small range of the displacement, the relationship between the output intensity and displacement is linear. Therefore, at a proper operating frequency, this structure can be utilized as a micro-displacement sensor with the high sensitivity. The transmission coefficients for different frequencies can be expressed approximately as the following Lorentzian function [2, 9]:

$$T(\omega, \omega_0) = \frac{(\omega_0/2Q)^2}{(\omega - \omega_0)^2 + (\omega_0/2Q)^2} \quad (1)$$

where  $\omega_0$  is the resonant frequency, and  $Q$  is the quality factor of the resonant cavity. The resonant frequency  $\omega_0$  is shifted by changing the cavity length. The PhC cavity in this sensor is made by the green holes as shown in Fig. 1. When the movable segment is shifted along the common axis with a certain operating frequency  $\omega$ , we can then derive the variation of the transmission coefficient as

$$\Delta T(\Delta x) = T(x + \Delta x) - T(x) \quad (2)$$

where  $\Delta x$  is the displacement between two segments. By using Taylor series, we obtain [2]

$$\Delta T(\Delta x) = T'(x) \cdot \Delta x + \frac{T''(x)}{2} \cdot \Delta x^2 + O(\Delta x). \quad (3)$$

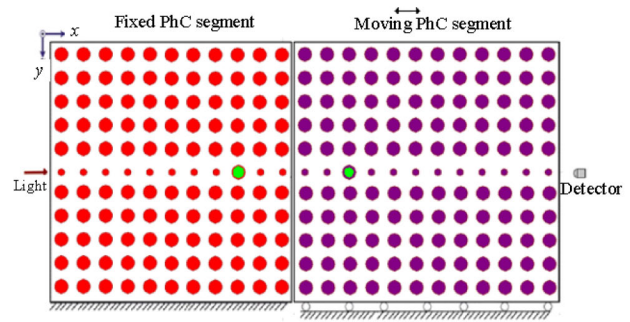


Fig. 1 Layout of the micro-displacement sensor based on the high sensitivity photonic crystal.

In practical systems, a proper operating frequency  $\omega$  should be selected to apply the sensor in the quasi-linear region [1]. Considering  $\omega_1$  which satisfies  $T''(\omega_0, \omega_1) \approx 0$ , then  $\Delta T(\Delta x)$  can be considered as the linear function as [2]:

$$S = \frac{\Delta T}{\Delta x}. \quad (4)$$

## 3. Sensor parameters and simulation results

As shown in Fig. 1, the micro-displacement sensor was designed in the 2D PhC with the square lattice of air holes in the dielectric. The radius of the holes was considered as  $0.2a$ . The dielectric constant was 11.56, therefore, the refractive index  $n$  can be calculated as

$$n = \sqrt{\epsilon} = \sqrt{11.56} = 3.4. \quad (5)$$

Each segment of the sensor was formed by  $11 \times 11$  holes in the dielectric. In this sensor, the line defect was created by shrinking a row rather than removing them, as shown in Fig. 1. This 2D PhC had a photonic band gap (PBG) only for TE modes [10]. Figure 2 shows the PBG for this sensor. As shown in Fig. 1, the waveguide created by changing the radius of holes was similar to the W1 waveguide, but the modes were shifted to the higher frequency inside the bandgap, because the refractive index of the structure decreased. This structure significantly increased the amount of the surface area available for sensing in the central high-field regions which caused an increase in the sensitivity [11, 12].

As shown in Fig. 2, this structure had two PBG ranges,  $0.325 \left[ \frac{a}{\lambda} \right] - 0.445 \left[ \frac{a}{\lambda} \right]$  and  $0.625 \left[ \frac{a}{\lambda} \right] - 0.675 \left[ \frac{a}{\lambda} \right]$ .

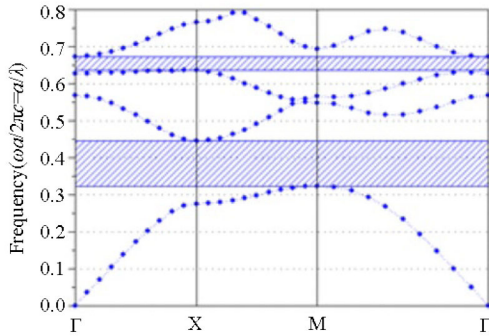


Fig. 2 Photonic band gap of the designed sensor.

We chose  $2.7 \mu\text{m}$  as the operating wavelength, because this wavelength was coincident with the cavity resonator wavelength. The frequency response of the structure is shown in Fig. 3. Therefore, the  $Q$ -factor can be calculated as

$$Q = \frac{\lambda}{\Delta\lambda} = \frac{2.725\mu\text{m}}{0.015\mu\text{m}} = 181. \quad (6)$$

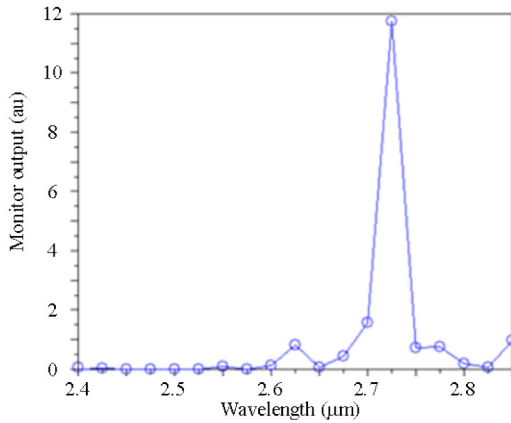


Fig. 3 Frequency response.

The wave propagation in the structure and the output intensity as a linear function of the displacement are shown in Figs. 4 and 5, respectively. According to Fig. 5, the variation of the transmission coefficient decreases from 3.2 to 1.4 when the displacement between two segments increases from  $0.0 \mu\text{m}$  to  $0.5 \mu\text{m}$ . In other regions, the relationship between the output intensity and displacement is not linear.

The sensitivity can be calculated by using data from Fig. 5 as

$$\text{Sensitivity} = \frac{3.2 - 1.4}{0.5\mu\text{m}} = 3.6 \mu\text{m}^{-1}. \quad (7)$$

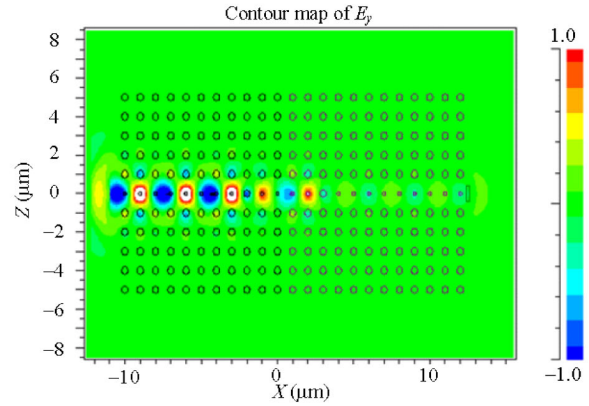


Fig. 4 Wave propagation in the designed sensor.

According to Fig. 5 for the displacement between 0 and  $0.5 \mu\text{m}$ , the regression coefficient is 0.981137, which implies that the sensor is working in a linear region. Table 1 shows the relationship between the displacement, sensitivity and regression. For the displacement between  $-0.5 \mu\text{m}$  and  $0.0 \mu\text{m}$ , the regression coefficient is lower than 0.5, therefore there is a nonlinear relation between the output intensity and displacement.

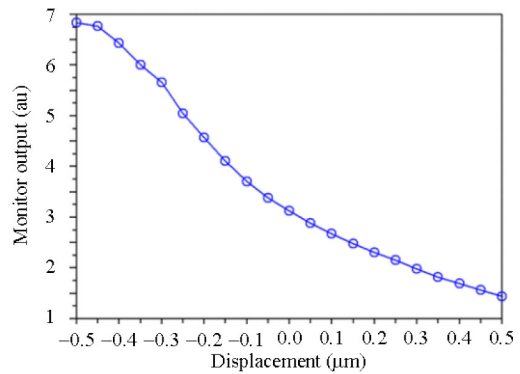


Fig. 5 Relationship between the output intensity and displacement.

If the radius of holes increases, the value of the relative refractive index of structure decreases, the photonic band gap shifts to the higher frequencies, and consequently the sensitivity increases [11]. But with an increase in the radius, the waveguide band gap can be overlapped with the structure band gap, and the sensor does not work in a linear mode.

Table 1 Sensitivity and regression for displacement regions.

Displacement ( $\mu\text{m}$ )	Sensitivity ( $\mu\text{m}^{-1}$ )	Regression
- 0.5 – - 0.4	4	0.5073377
- 0.4 – - 0.3	7.5	0.451036
- 0.3 – - 0.2	10.5	0.236934
- 0.2 – - 0.1	9	0.307377
- 0.1 – 0.0	5.5	0.190320
0.0 – 0.1	3.5	0.982480
0.1 – 0.2	3.5	0.909492
0.2 – 0.3	3.6	0.945725
0.3 – 0.4	3.6	0.986207
0.4 – 0.5	3.7	0.921880

As shown in Fig. 6(a) by increasing the radius of holes, the sensitivity increases, but as shown in Fig. 6(b), the regression has a maximum value in the radius of holes equal to  $0.50\mu\text{m}$ . By selecting the radius of holes between  $0.49\mu\text{m}$  and  $0.51\mu\text{m}$ , the sensitivity and regression are optimum.

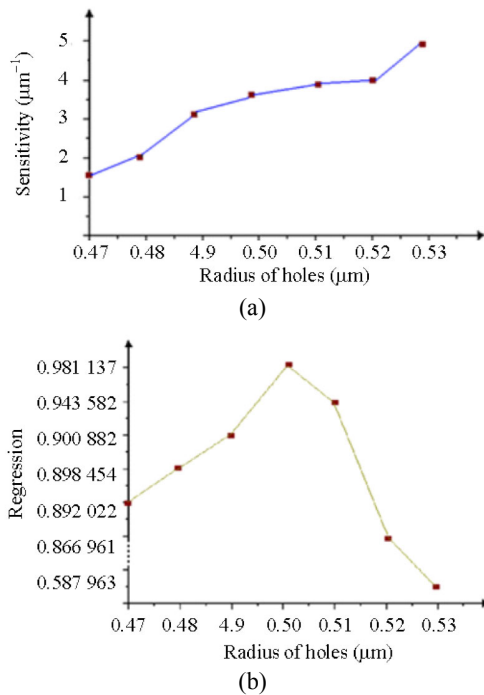


Fig. 6 Effect of increasing the radius of holes on the (a) sensitivity and (b) regression.

Table 2 describes a brief comparison between the results obtained from the similar structures reported in [1–3, 8] and presented sensor in this paper. As shown in this table, the designed sensor has a higher sensitivity in a wide measurement range.

Table 2 Brief comparison between the results of the presented sensor and reported sensors in [1–3, 8].

Displacement sensor	Q-factor	Sensitivity ( $\mu\text{m}^{-1}$ )	Displacement ( $\mu\text{m}$ )
Displacement sensing using photonic crystal waveguides [3]		1	0.0 – 0.2
Sensor based on line-defect resonant cavity in photonic crystal [1]	40	1.25	0.0 – 0.2
Micro-displacement sensor with large dynamic range based on photonic crystal co-directional coupler [8]		1	Limited by the length of the sensor
Micro-displacement sensor based on high-Q nanocavity in slot photonic crystal [2]	6000	1	0.0 – 0.2
Presented sensor	180	3.8	0.0 – 0.5

### 4. Conclusions

In this paper, we introduce a micro-displacement sensor based on the 2D photonic crystal. The 2D PhC consisted of air holes in the dielectric with the square lattice structure. In this sensor, by selecting the appropriate operating frequency, the sensitivity was obtained as  $3.6\mu\text{m}^{-1}$  –  $3.8\mu\text{m}^{-1}$  depending on the different radii of holes, and the Q-factor of the resonant cavity was calculated nearly 180. The linear region of the sensitivity was obtained in the range of  $0.0\mu\text{m}$  –  $0.5\mu\text{m}$ . Therefore, at a proper operating frequency, this structure can be used as a micro-displacement sensor with the high sensitivity and large measurement range. Compared to the similar structures reported in [1–3, 8], the designed sensor has a higher sensitivity and a wider measurement range.

### Acknowledgment

The authors would like to thank anonymous reviewers for their helpful and constructive comments and recommendations.

**Open Access** This article is distributed under the terms of the Creative Commons Attribution License which permits any use, distribution, and reproduction in any medium, provided the original author(s) and source are credited.

## References

- [1] Z. Xu, L. Cao, C. Gu, Q. He, and G. Jin, "Micro-displacement sensor based on line-defect resonant cavity in photonic crystal," *Optics Express*, 2006, 14(1): 298–305.
- [2] D. Yang, H. Tian, and Y. Ji, "Micro-displacement sensor based on high- $Q$  nanocavity in slot photonic crystal," *Optical Engineering*, 2011, 50(5): 544021–544026.
- [3] O. Levy, B. Z. Steinberg, M. Nathan, and A. Boag, "Ultrasensitive displacement sensing using photonic crystal waveguides," *Applied Physics Letters*, 2005, 86(10): 104102–104104.
- [4] S. Olyaei, S. Hamedi, and Z. Dashtban, "Design of electronic sections for nano-displacement measuring system," *Frontiers of Optoelectronics in China*, 2010, 3(4): 376–381.
- [5] S. Olyaei and S. M. Nejad, "Design and simulation of velocity and displacement measurement system with subnanometer uncertainty based on a new stabilized laser Doppler-interferometer," *The Arabian Journal for Science and Engineering*, 2007, 32(2C): 89–99.
- [6] S. Olyaei and A. A. Dehghani, "High resolution and wide dynamic range pressure sensor based on two-dimensional photonic crystal," *Photonic Sensors*, 2012, 2(1): 92–96.
- [7] S. Olyaei, A. Naraghi, and V. Ahmadi, "High sensitivity evanescent-field gas sensor based on modified photonic crystal fiber for gas condensate and air pollution monitoring," *Optik*, 2014, 125(1): 596–600.
- [8] Z. Xu, L. Cao, P. Su, Q. He, G. Jin, and G. Gu, "Micro-displacement sensor with large dynamic range based on photonic crystal co-directional coupler," *IEEE Journal of Quantum Electronics*, 2007, 43(2): 182–187.
- [9] H. A. Haus, *Wave and fields in optoelectronics (Prentice-Hall Series in Solid State Physical Electronics)*, Englewood Cliffs, USA: Prentice Hall, 1985: 258–273.
- [10] J. D. Joannopoulos, S. G. Johnson, J. N. Winn, and R. D. Meade, *Photonic Crystals Molding the Flow of Light*, Princeton: Princeton University Press, 2007.
- [11] S. C. Buswell, V. A. Wright, J. M. Buriak, V. Van, and S. Evoy, "Specific detection of proteins using photonic crystal waveguides," *Optics Express*, 2008, 16(20): 15949–15957.
- [12] F. Bougrioua, T. Boumazab, and M. Bouchemat, "Design of photonic crystals waveguide using microfluidic infiltration," *Applied Mechanics and Materials*, 2014, 492: 301–305.